# Narrow Line Seyfert 1 galaxies in the context of Quasar Main Sequence

Bożena Czerny

*Center for Theoretical Physics, Warsaw*

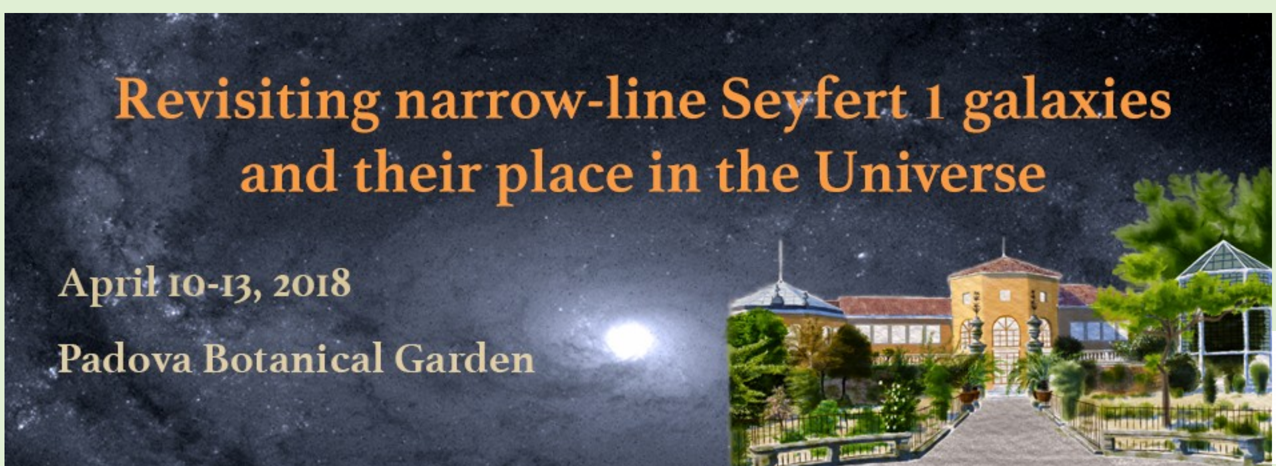


NARODOWE CENTRUM NAUKI

# Two old concepts:

***Narrow Line Seyfert 1***

***Quasar Main Sequence***
***Eigenvector 1***

***Do they tell us the same story?***

# Narrow Line Seyfert 1

Introduced in 1985 by Osterbrock & Pogge

**Definition:**
- Intensity ratios  OIII]5007/Hbeta < 3
- Line widths below 1000 km/s in original paper, later widely adopted 2000 km/s limit.

**Interpretation:**
- These sources do have a dense BLR part independently from normal low density NLR (forbidden lines)
- They represent a tail of the trend od decreasing EW(Hbeta) with Hbeta line width.

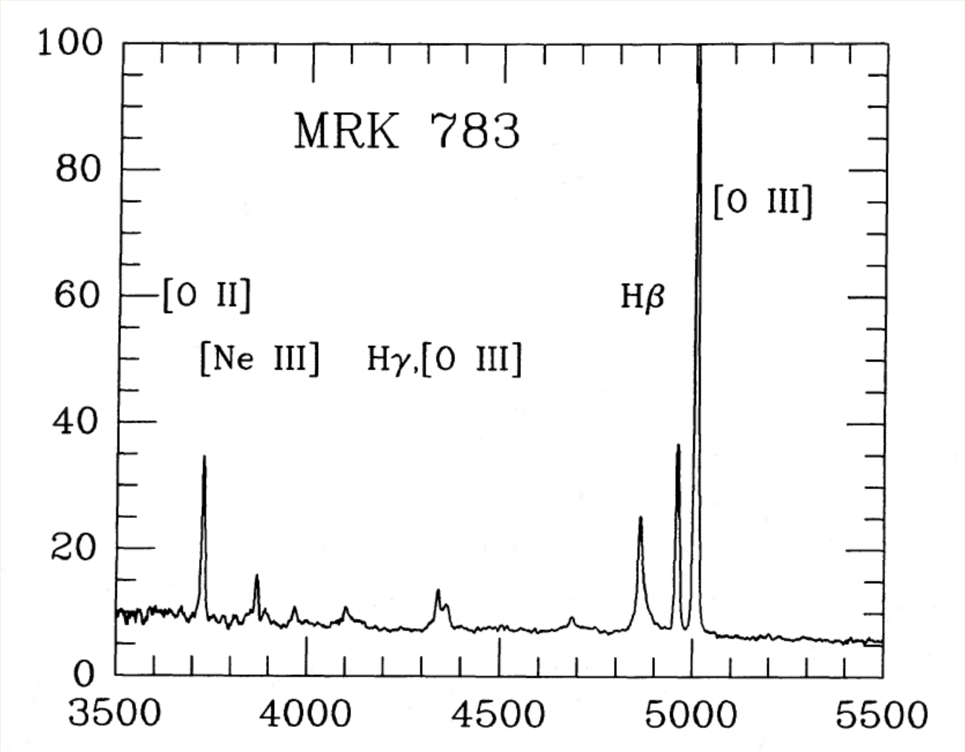


*Example from original Osterbrock & Pogge*

# Narrow Line Seyfert 1

Interpretation through basic theoretical parameters:

1995: Pounds et al. NLS1 are **high Eddington ratio sources.**

Mon. Not. R. Astron. Soc. **277,** L5–L10 (1995)

**RE 1034 + 39: a high-state Seyfert galaxy?**

K. A. Pounds,[1] C. Done[2] and J. P. Osborne[1]

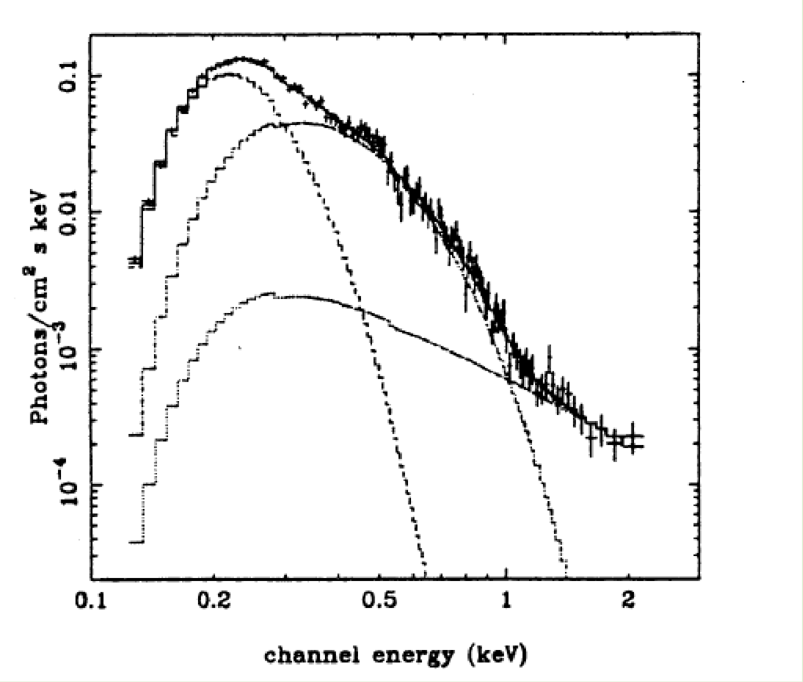

# Eigenvector 1 and the quasar main sequence

Introduced in 1992 by Boroson & Green

**Definition:**
A combination of 13 parameters, including R_Fe = EW(FeII)/EW(Hbeta)

TABLE 3

LINE AND CONTINUUM CORRELATION MATRIX

| | z | $M_V$ | Log R | $\alpha_{ox}$ | EW H$\beta$ | EW $\lambda$5007 | EW $\lambda$4686 | EW Fe II | R $\lambda$5007 | R $\lambda$4686 | R Fe II | Peak $\lambda$5007 | H$\beta$ FWHM | H$\beta$ shift | H$\beta$ shape | H$\beta$ asymm | $M_{[OIII]}$ |
|---|---|---|---|---|---|---|---|---|---|---|---|---|---|---|---|---|---|
| z | | −0.871 | 0.252 | 0.238 | −0.083 | −0.180 | −0.419 | −0.128 | −0.156 | −0.442 | −0.134 | 0.098 | 0.307 | 0.031 | 0.228 | −0.171 | −0.554 |
| $M_V$ | −0.871 | | −0.376 | −0.229 | 0.053 | 0.289 | 0.588 | 0.050 | 0.267 | 0.612 | 0.098 | 0.025 | −0.275 | −0.076 | −0.191 | 0.104 | 0.650 |
| Log R | 0.252 | −0.376 | | −0.088 | −0.145 | 0.200 | −0.146 | −0.404 | 0.292 | −0.128 | −0.319 | 0.364 | 0.303 | 0.237 | 0.052 | −0.273 | −0.540 |
| $\alpha_{ox}$ | 0.238 | −0.229 | −0.088 | | −0.318 | −0.413 | −0.358 | 0.132 | −0.261 | −0.301 | 0.209 | −0.319 | −0.086 | 0.165 | 0.328 | 0.225 | 0.075 |
| EW H$\beta$ | −0.083 | 0.053 | −0.145 | −0.318 | | 0.363 | 0.324 | 0.142 | −0.103 | −0.010 | −0.425 | 0.065 | 0.181 | −0.149 | −0.088 | −0.185 | −0.188 |
| EW $\lambda$5007 | −0.180 | 0.289 | 0.200 | −0.413 | 0.363 | | 0.488 | −0.389 | 0.803 | 0.311 | −0.462 | 0.716 | 0.136 | −0.029 | −0.197 | −0.239 | −0.345 |
| EW $\lambda$4686 | −0.419 | 0.588 | −0.146 | −0.358 | 0.324 | 0.488 | | −0.077 | 0.355 | 0.876 | −0.222 | 0.271 | −0.199 | −0.120 | −0.167 | −0.119 | 0.165 |
| EW Fe II | −0.128 | 0.050 | −0.404 | 0.132 | 0.142 | −0.389 | −0.077 | | −0.529 | −0.084 | 0.766 | −0.670 | −0.436 | −0.155 | 0.122 | 0.454 | 0.494 |
| R $\lambda$5007 | −0.156 | 0.267 | 0.292 | −0.261 | −0.103 | 0.803 | 0.355 | −0.529 | | 0.347 | −0.365 | 0.827 | 0.139 | 0.010 | −0.113 | −0.288 | −0.361 |
| R $\lambda$4686 | −0.442 | 0.612 | −0.128 | −0.301 | −0.010 | 0.311 | 0.876 | −0.084 | 0.347 | | −0.042 | 0.181 | −0.288 | −0.053 | −0.140 | −0.039 | 0.270 |
| R Fe II | −0.134 | 0.098 | −0.319 | 0.209 | −0.425 | −0.462 | −0.222 | 0.766 | −0.365 | −0.042 | | −0.635 | −0.548 | −0.001 | 0.198 | 0.591 | 0.604 |
| Peak $\lambda$5007 | 0.098 | 0.025 | 0.364 | −0.319 | 0.065 | 0.716 | 0.271 | −0.670 | 0.827 | 0.181 | −0.635 | | 0.508 | −0.003 | −0.121 | −0.472 | −0.555 |
| H$\beta$ FWHM | 0.307 | −0.275 | 0.303 | −0.086 | 0.181 | 0.136 | −0.199 | −0.436 | 0.139 | −0.288 | −0.548 | 0.508 | | −0.068 | −0.146 | −0.316 | −0.450 |
| H$\beta$ shift | 0.031 | −0.076 | 0.237 | 0.165 | −0.149 | −0.029 | −0.120 | −0.155 | 0.010 | −0.053 | −0.001 | −0.003 | −0.068 | | 0.130 | 0.119 | −0.011 |
| H$\beta$ shape | 0.228 | −0.191 | 0.052 | 0.328 | −0.088 | −0.197 | −0.167 | 0.122 | −0.113 | −0.140 | 0.198 | −0.121 | −0.146 | 0.130 | | 0.066 | −0.028 |
| H$\beta$ asymm | −0.171 | 0.104 | −0.273 | 0.225 | −0.185 | −0.239 | −0.119 | 0.454 | −0.288 | −0.039 | 0.591 | −0.472 | −0.316 | 0.119 | 0.066 | | 0.481 |
| $M_{[OIII]}$ | −0.554 | 0.650 | −0.540 | 0.075 | −0.188 | −0.345 | 0.165 | 0.494 | −0.361 | 0.270 | 0.604 | −0.555 | −0.450 | −0.011 | −0.028 | 0.481 | |

# Quasar Main Sequence – optical plane

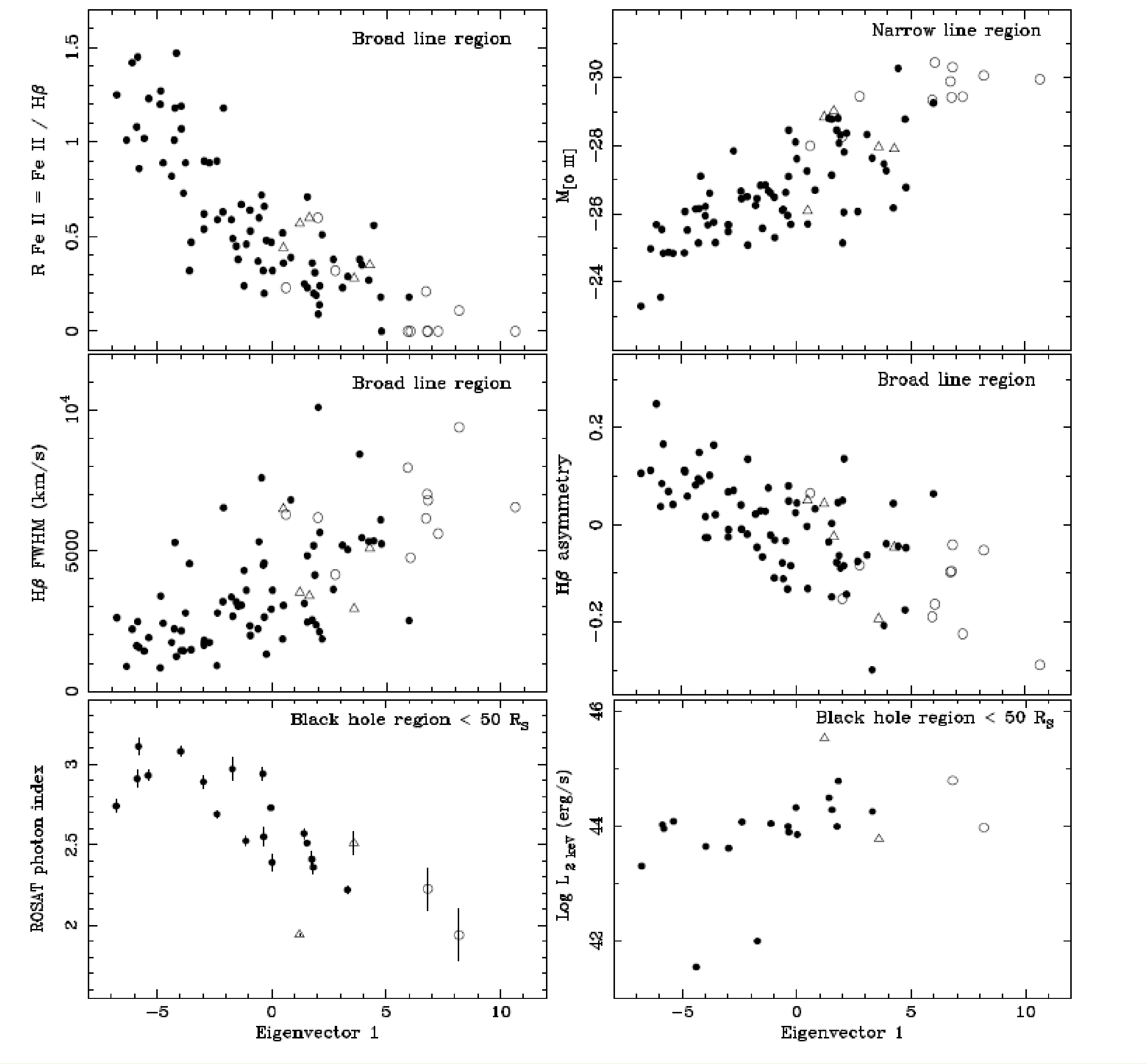


Tight correlation between EV1 and R_Fe allows to reduce EV1 analysis to the optical plane...

*Brandt & Boller 1997*

# Quasar Main Sequence – optical plane

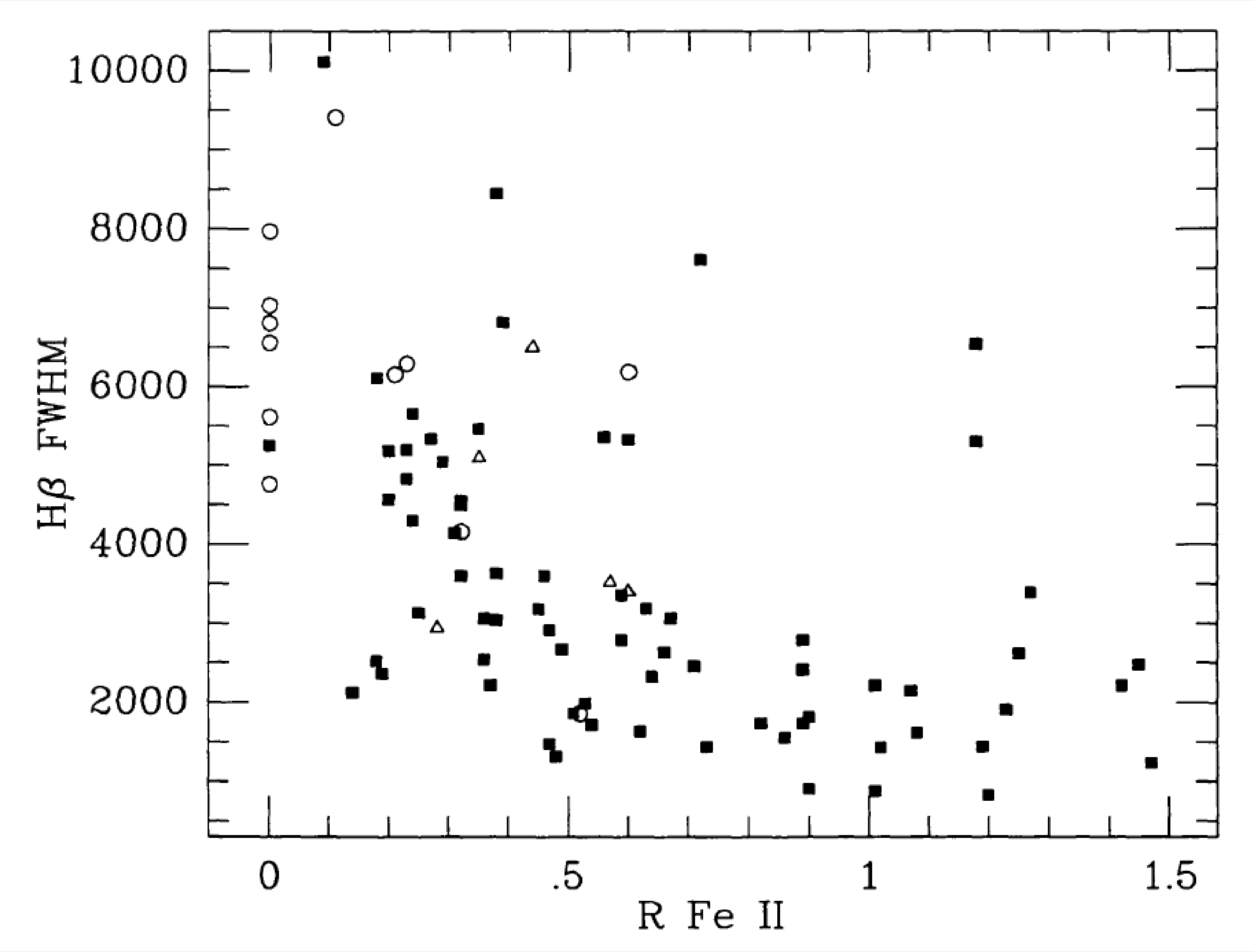


Tight correlation between EV1 and R_Fe allows to reduce EV1 analysis to the optical plane...

*Boroson & Green 1992*

# Eigenvector 1 and the quasar main sequence

Interpretation through basic theoretical parameters:

1992, Boroson & Green: Eddington ratio is the main driver of the EV1, so **high Eddington ratio sources are located at the far end of the sequence,** where high Eddington ratio sources lie among strong Fe II emitters.

| Property | Eigenvector 1 29.2% |
| --- | --- |
| $M_V$ ........... | −0.269 |
| Log $R$ ........ | +0.566 |
| $\alpha_{ox}$ ........... | −0.340 |
| EW Hβ ....... | +0.265 |
| $R$ λ5007 ...... | +0.598 |
| $R$ λ4686 ...... | −0.033 |
| $R$ Fe II ........ | −0.832 |
| Peak λ5007 ... | +0.845 |
| Hβ FWHM ... | +0.654 |
| Hβ shift ....... | −0.025 |
| Hβ shape ..... | −0.173 |
| Hβ asymm .... | −0.679 |
| $M_{[O\ III]}$ ......... | −0.811 |

*Correlations of EV1 with line and continuum properties in Boroson & Green*

# Quasar Main Sequence – optical plane

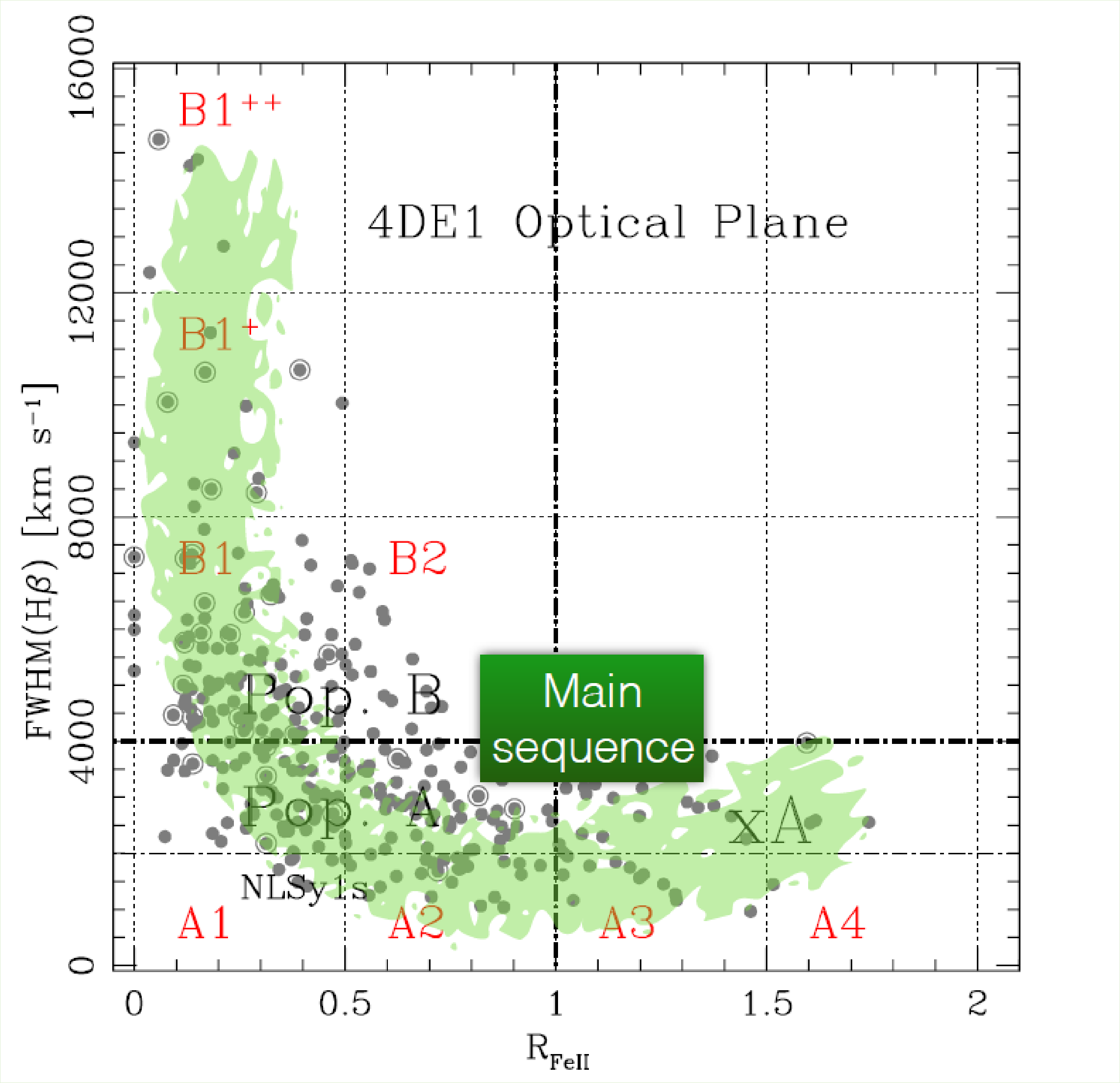


A lot of later studies were made along these line. More modern versions contain more pooints.

*Marziani et al. 2018*

# Quasar Main Sequence optical plane: 2000 vs 4000 km/s

Here the classification of sources into type A and B has been done at 4000 km/s, following Sulentic et al. (2000) instead of customary 2000 km/s for NLS1.

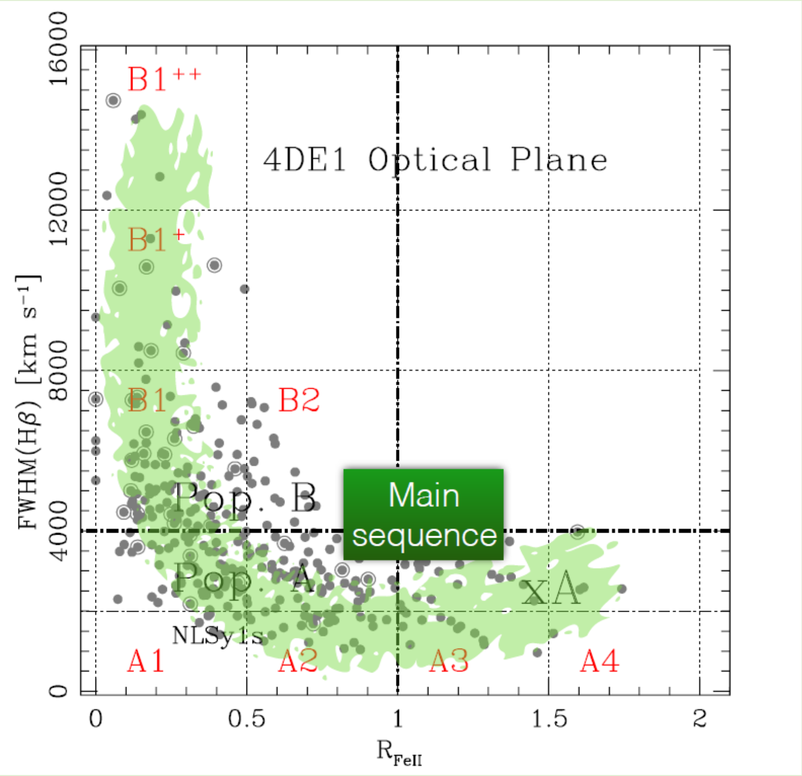


*Marziani et al. 2018*

For me, as a theoretician, this is simple: 2000 km/s is apppropriate for low black hole mass sources (Seyfert galaxies), 4000 km/s are appropriate for high black hole mass sources (quasars).

If the division between classes is connected to a fixed the Eddington ratio, and the line width scales with mass and R_BLR which in turn scales with the monochromatic luminosity then SS accretion disk model implies

**V_limit propto M_BH^{1/6}**

Which takes us from 2000 km/s for 10^7 Ms to 4300 km/s for 10^9 Ms.

# NLS1 vs Quasar Main Sequence

1. NLS1 sources are believed to be high Eddington ratio sources

2. EV1 is supposed to be driven by the Eddington ratio, i.e. high Fe II emitters should be high Eddington ratio sources

**BUT**

galaxies. Some, in particular Mrk 493 and Mrk 42, have relatively strong Fe II emission; in others, especially Mrk 359, 783, and 1126, it is quite weak.

From the Astract of Osterbrock & Pogge (1985)

# So where do we have high Eddington ratio sources?

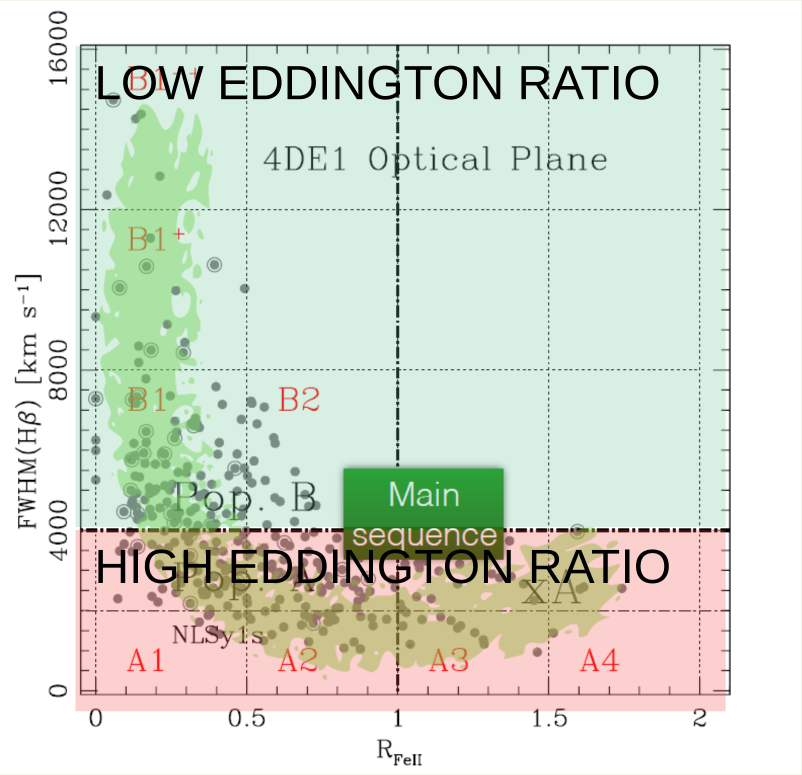


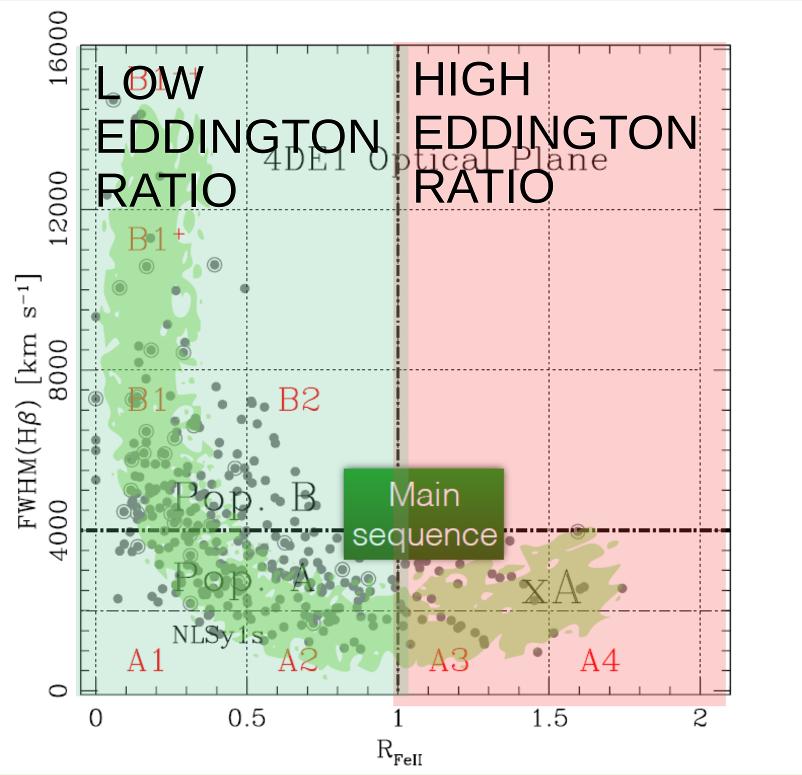


If NLS1/type A are all high L/L_EDD sources

If strong Fe II emitters are all high L/L_EDD sources

# Six examples of strong Fe II emitters

We selected 27 extreme cases of strong Fe II emitters with high quality data from Shen et al. (2011), and refitted them again. Six of them still have R_Fe > 1.3

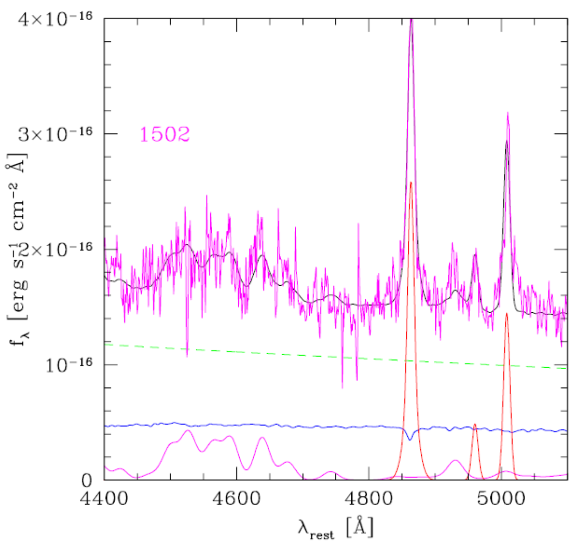


**Fig. 4.** The expanded region of the H$\beta$ line of the source SDSS150245.36+405437.2 (magenta line) which shows an ex-

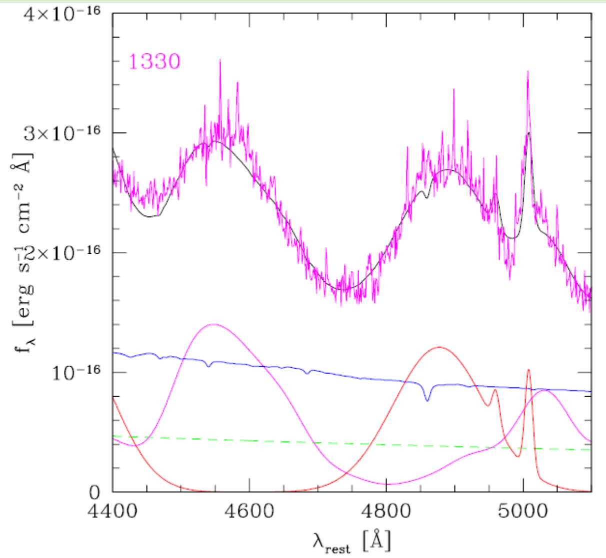


**Fig. 6.** The expanded region of the H$\beta$ line of the source SDSS133005.71+254243.7 (magenta line) which shows an ex-

*Sniegowska et al. (2018)*

***Three of the objects have FWHM > 4500 km/s, have low Eddington ratios***

***Three of the objects have FWHM < 2100 km/s, have high Eddington ratios***

# X-ray view

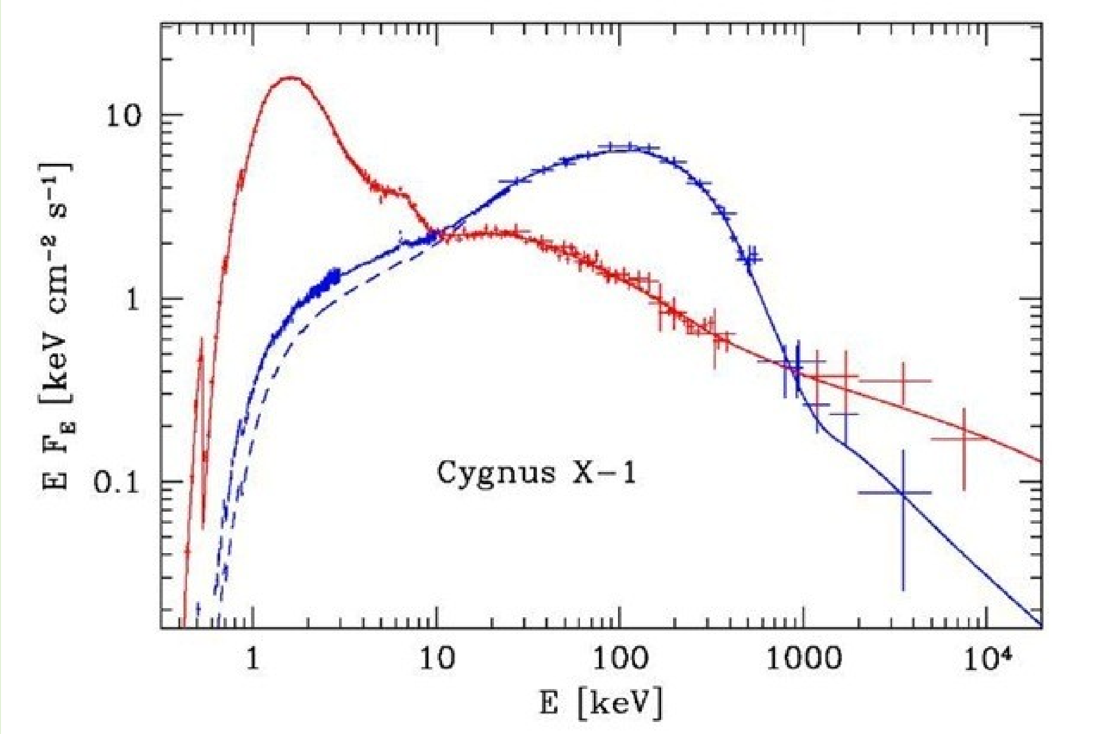


Galactic sources like Cygnus X-1 tell us that when the source is brighter the coronal X-ray emission is steeper Gierlinski et al 1999).

Figure from Brandt, Mathur & Elvis (1997) shows indeed a division in the X-ray slope at around 2000 km/s.

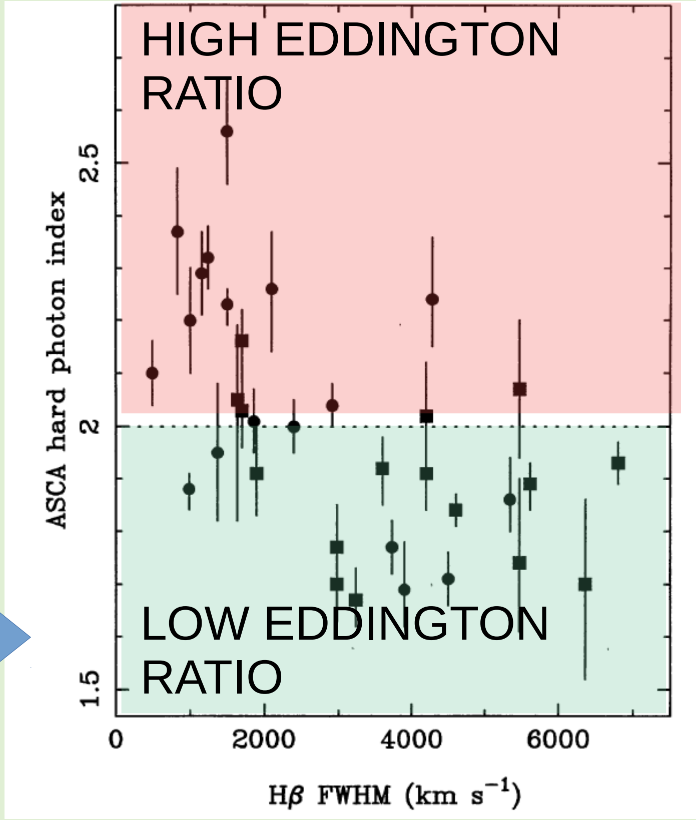


Weak Fe II emitters always have flat spectra, but strong Fe II emitters can be either flat or steep in ROSAT (Lawrence et al. 1997). But they are always X-ray weak.

# X-ray view

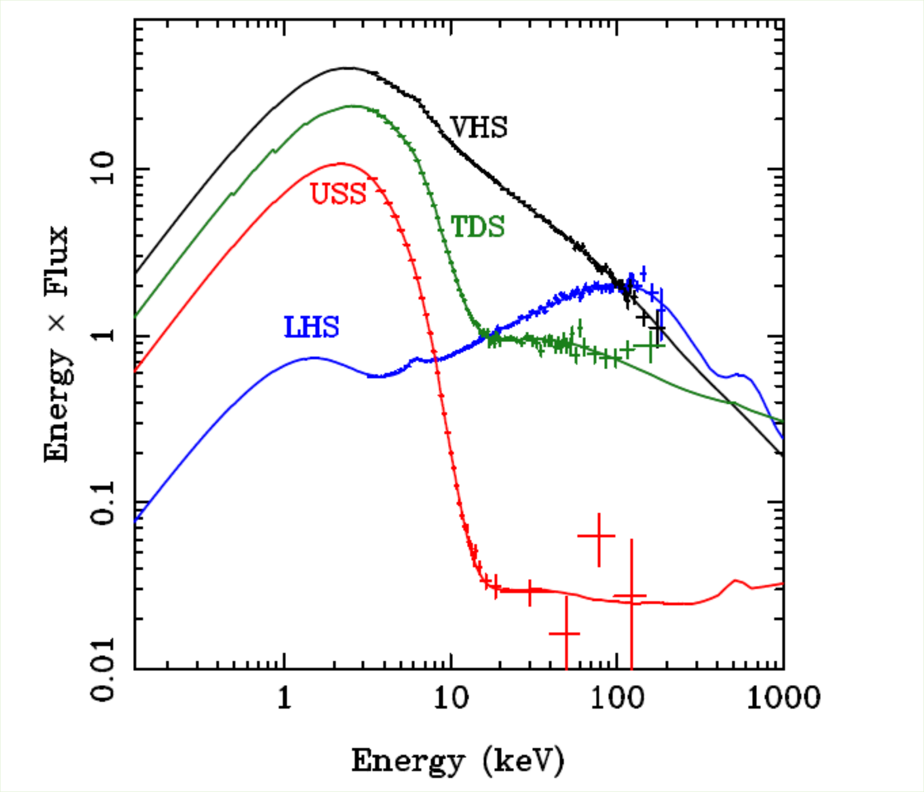


We should rather look at more typical galactic sources covering broader parameter rangge: here states from outburst of GRO J1655-40 (Done et al. 2007).

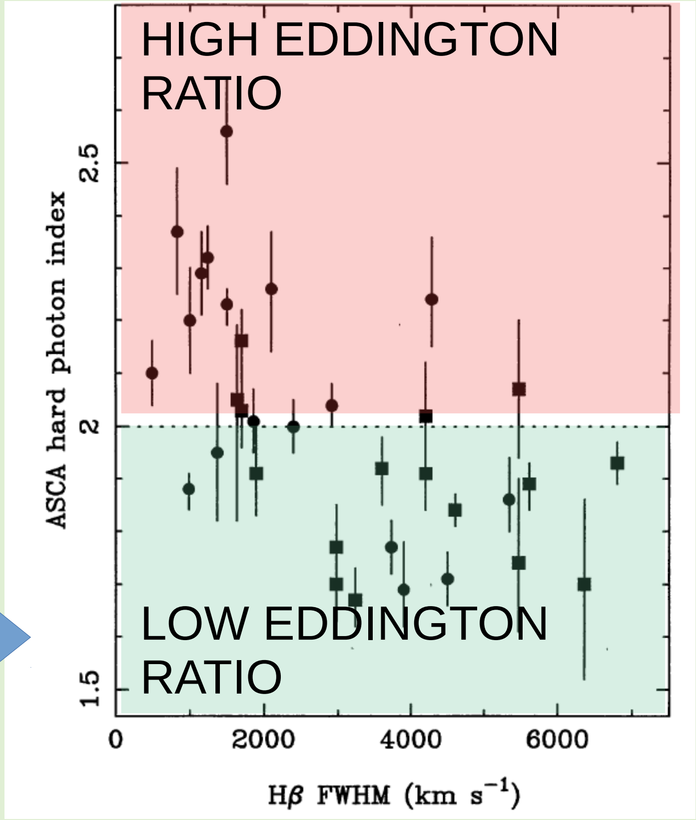


Figure from Brandt, Mathur & Elvis (1997) shows indeed a division in the X-ray slope at around 2000 km/s.

Weak Fe II emitters always have flat spectra, but strong Fe II emitters can be either flat or steep in ROSAT (Lawrence et al. 1997). But they are always X-ray weak.

# Problematic regions remain...

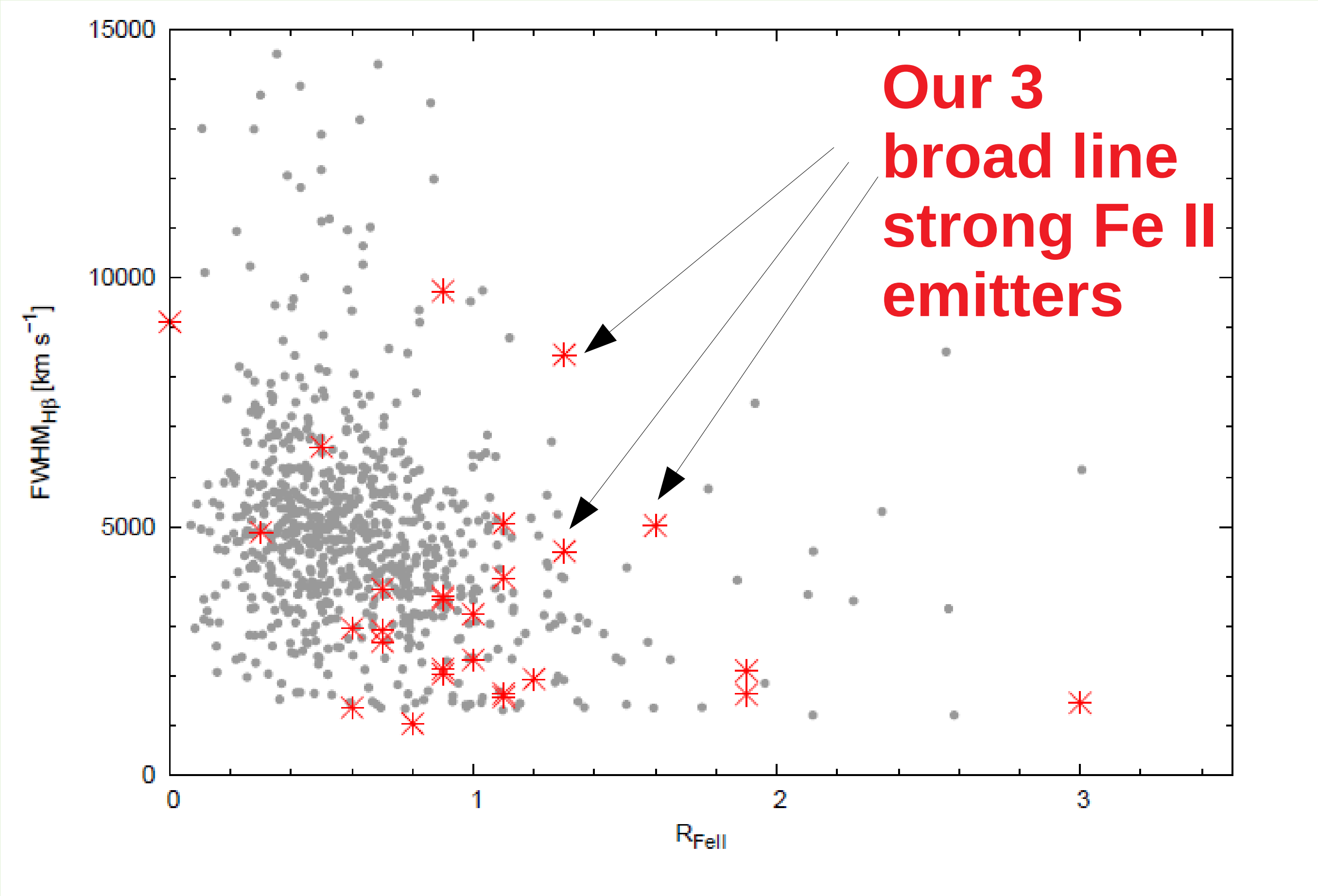


**These sources have L/L_Edd ratio below 0.03**

*Śniegowska et al. 2018*

# NLS1 impostors

Particularly RL NLS1 objects may beactually top view sources, and then only spectropolarimetry can reveil their nature (see talk by Luca Popovic).

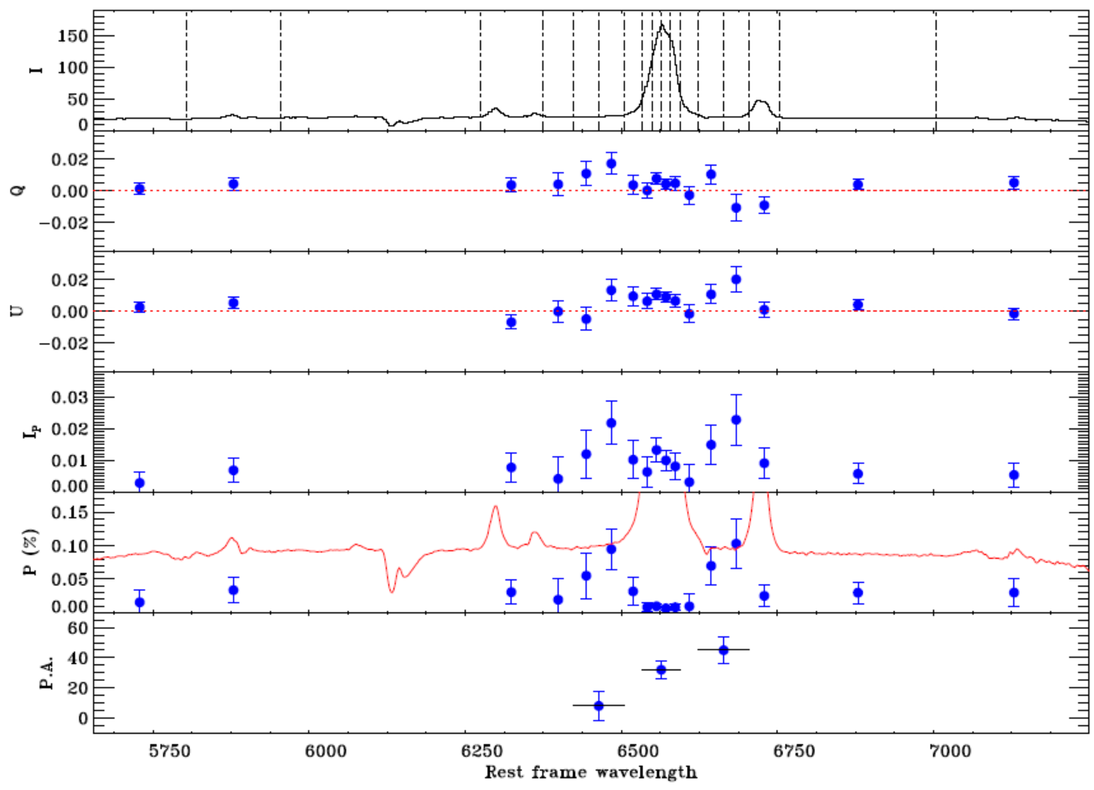


Figure 1. Top three panels: Stokes parameters of the PKS 2004-447 spectrum. Wavelengths are shown in rest frame in Å, fluxes are in arbitrary units because

Extreme example: Baldi et al. (2016)

In polarized light FWHM of the Halpha line went up to

**9000 km/s**

although in unpolarized light the source is classified as NLS1!

However, in most cases the incedent angle effect is not that large (20 deg vs. 40 deg)

# Black hole mass measurement and bolometric corrections

Black hole mass measurement in (some ?) NLS1 is not necessarily simple and reliable.

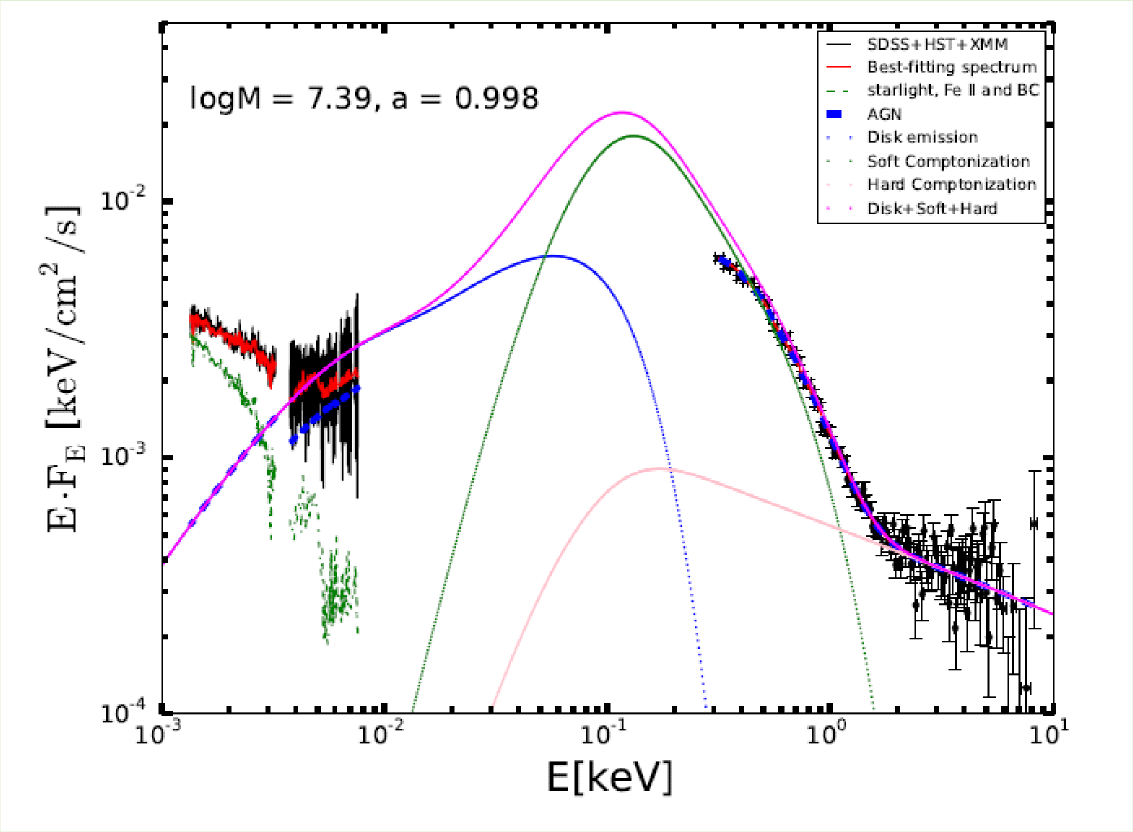


An example of broad band fit of RE J1034+397 from Czerny et al. 2016

# Black hole mass measurement and bolometric corrections

Black hole mass measurement in (some ?) NLS1 is not necessarily simple and reliable.

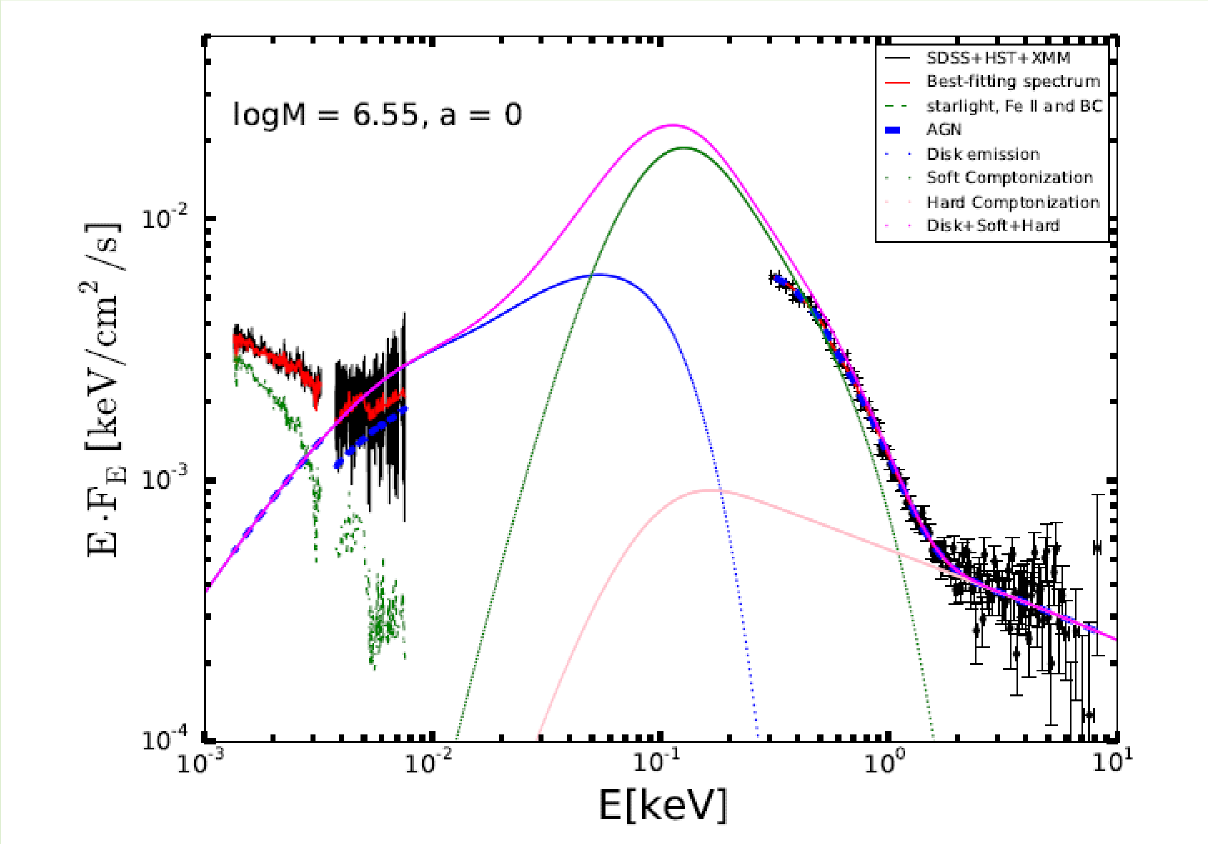


An example of broad band fit from Czerny et al. 2016

# Black hole mass measurement and bolometric corrections

Black hole mass measurement in (some ?) NLS1 is not necessarily simple and reliable.

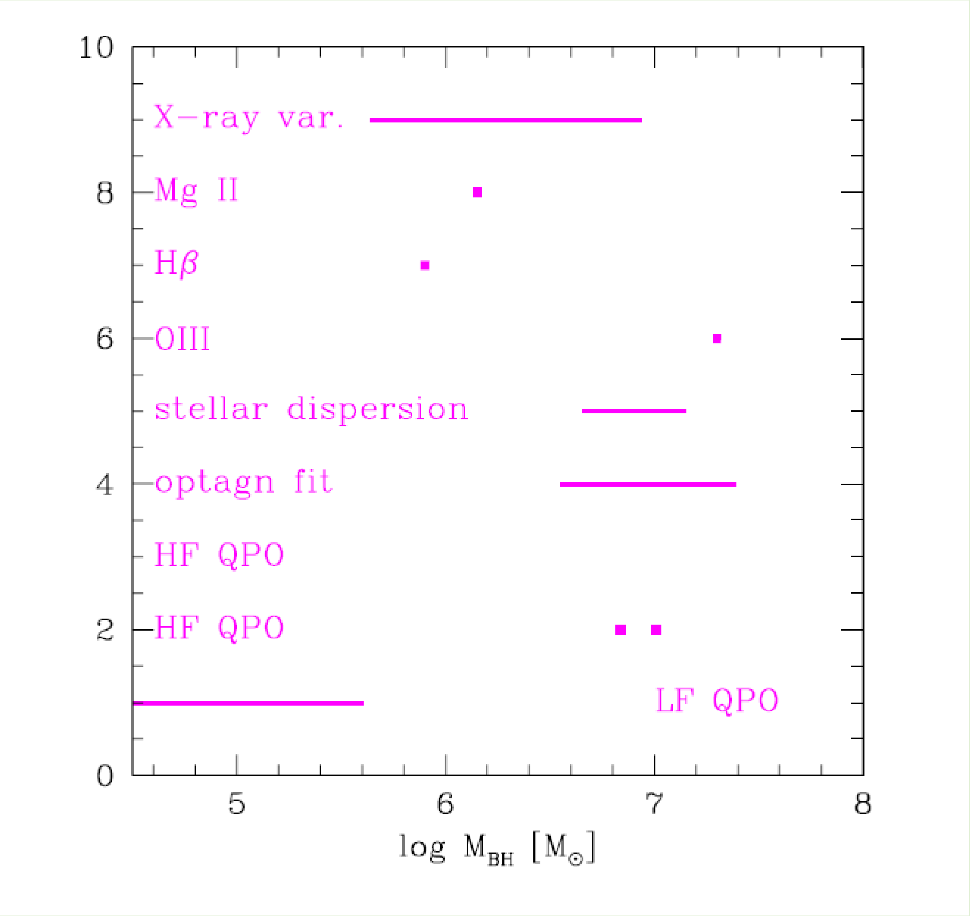


Now using many methods for this J1034+397 from Czerny et al. 2016

Reverberation was not yet done for this source but it is under way (SEAMBH project, Lijiang)

# X-ray excess variance

Advantage: should not be inclination-dependent
Disadvantage: unclear dependence on the accretion rate

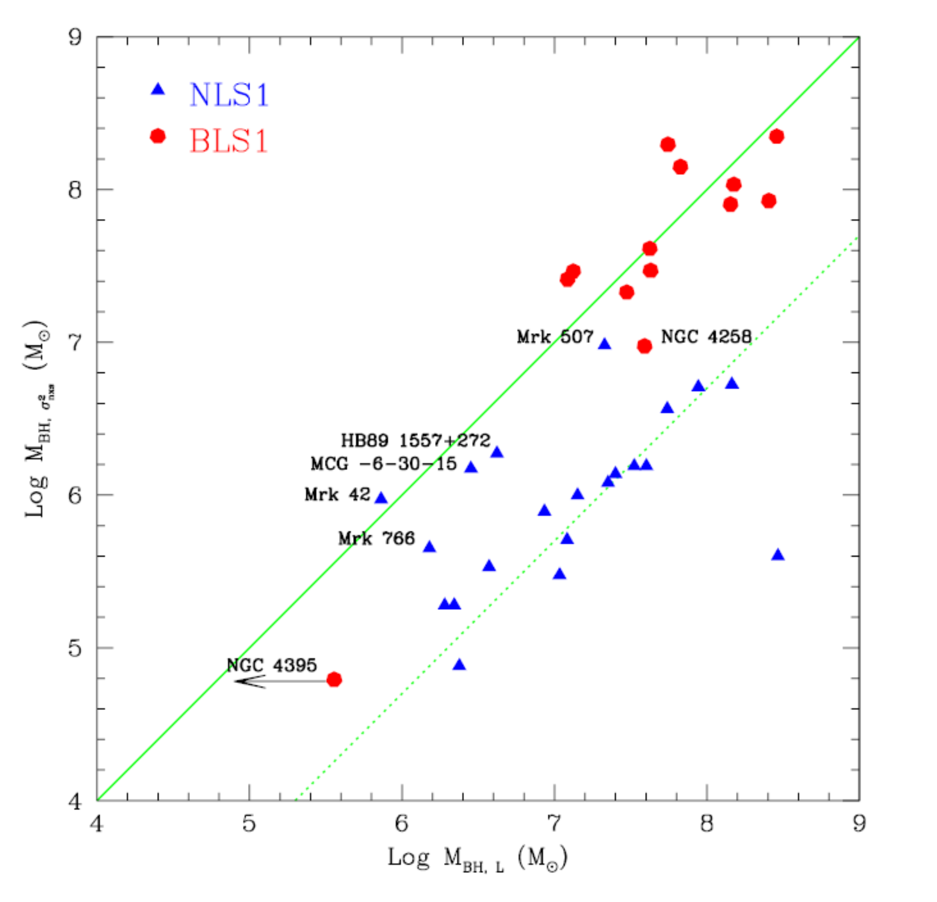


Nikolajuk et al. 2009

# Our theoretical approach

**Hypothesis: EV1 is driven by the SED shape**

**Realization:**

Modelling the Fe II and Hbeta production using recent version of CLOUDY code

Simple one zone production, constant density cloud, no shielding

Broad band spectrum: two component spectrum (Big Blue Bump + hard X-ray component), the relative normalization given by the Lusso & Risaliti (2017) phenomenological scaling, R_BLR from Bentz et al. (2013) scaling.

**Parameters: T_max, L/L_Edd, n**

# Modelled EV1 trend

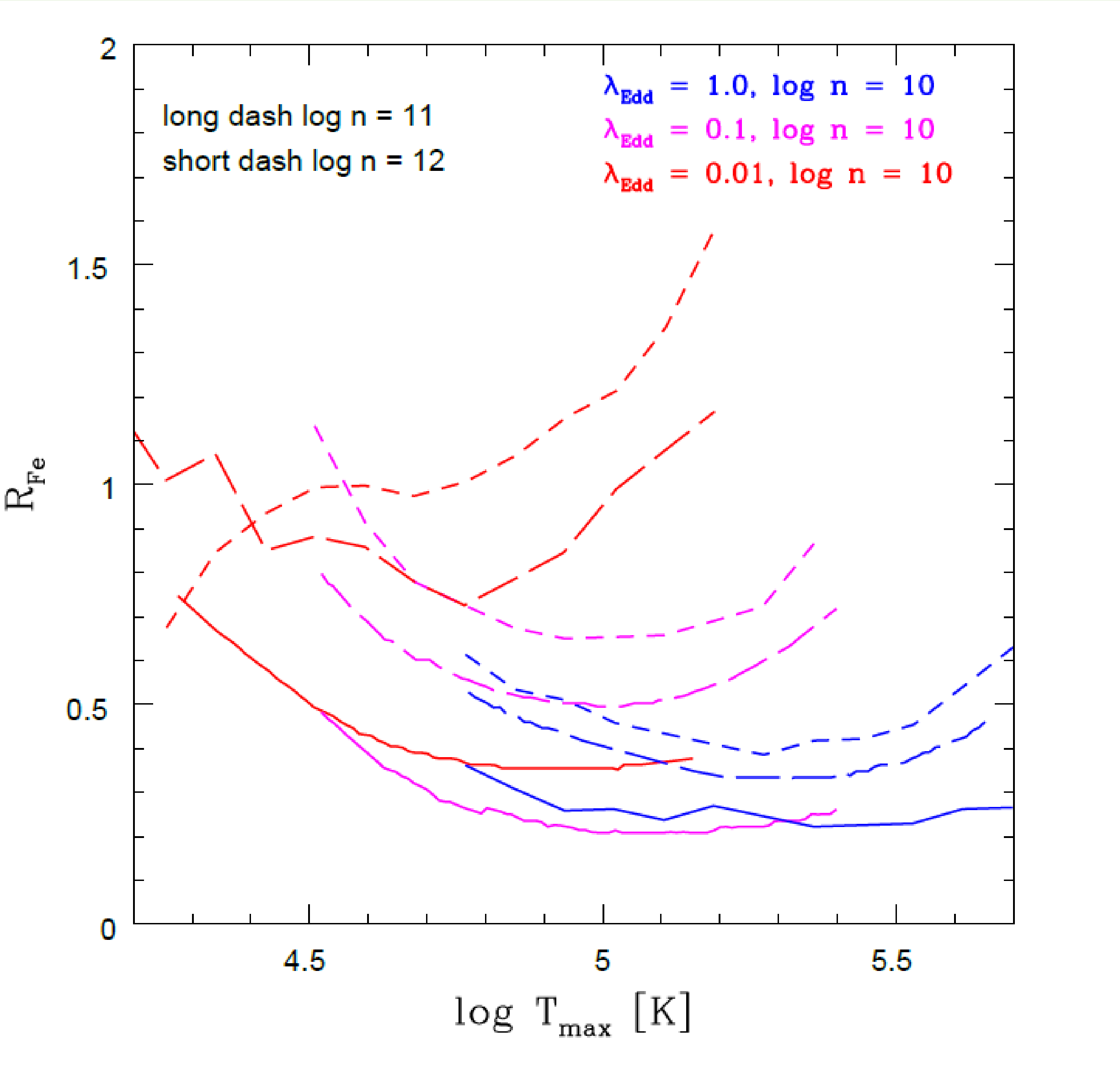


Mean quasar parameters (high quality subsample) from SDSS Shen et al. (2011) catalog are well represented:

Mean M_BH =8.4
Mean R_Fe = 0.64
Median R_Fe = 0.38

Corresponds to
Mean T_max = 4.80

*Panda et al. (in preparation)*

# Modelled EV1 trend

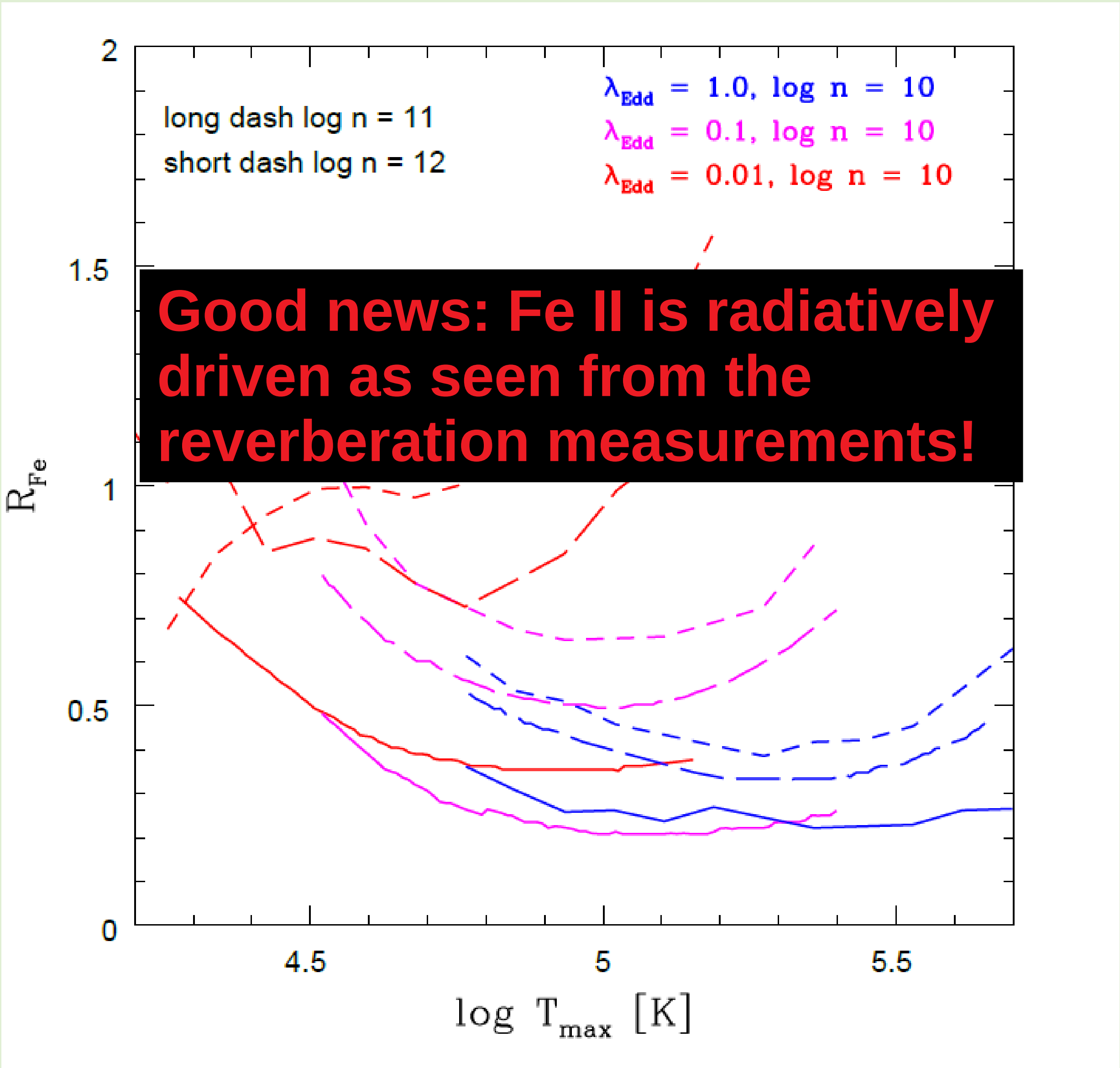


**Good news: Fe II is radiatively driven as seen from the reverberation measurements!**

Mean quasar parameters (high quality subsample) from SDSS Shen et al. (2011) catalog are well represented:

Mean M_BH =8.4
Mean R_Fe = 0.64
Median R_Fe = 0.38

Corresponds to
Mean T_max = 4.80

*Panda et al. (in preparation)*

# Modelled EV1 trend

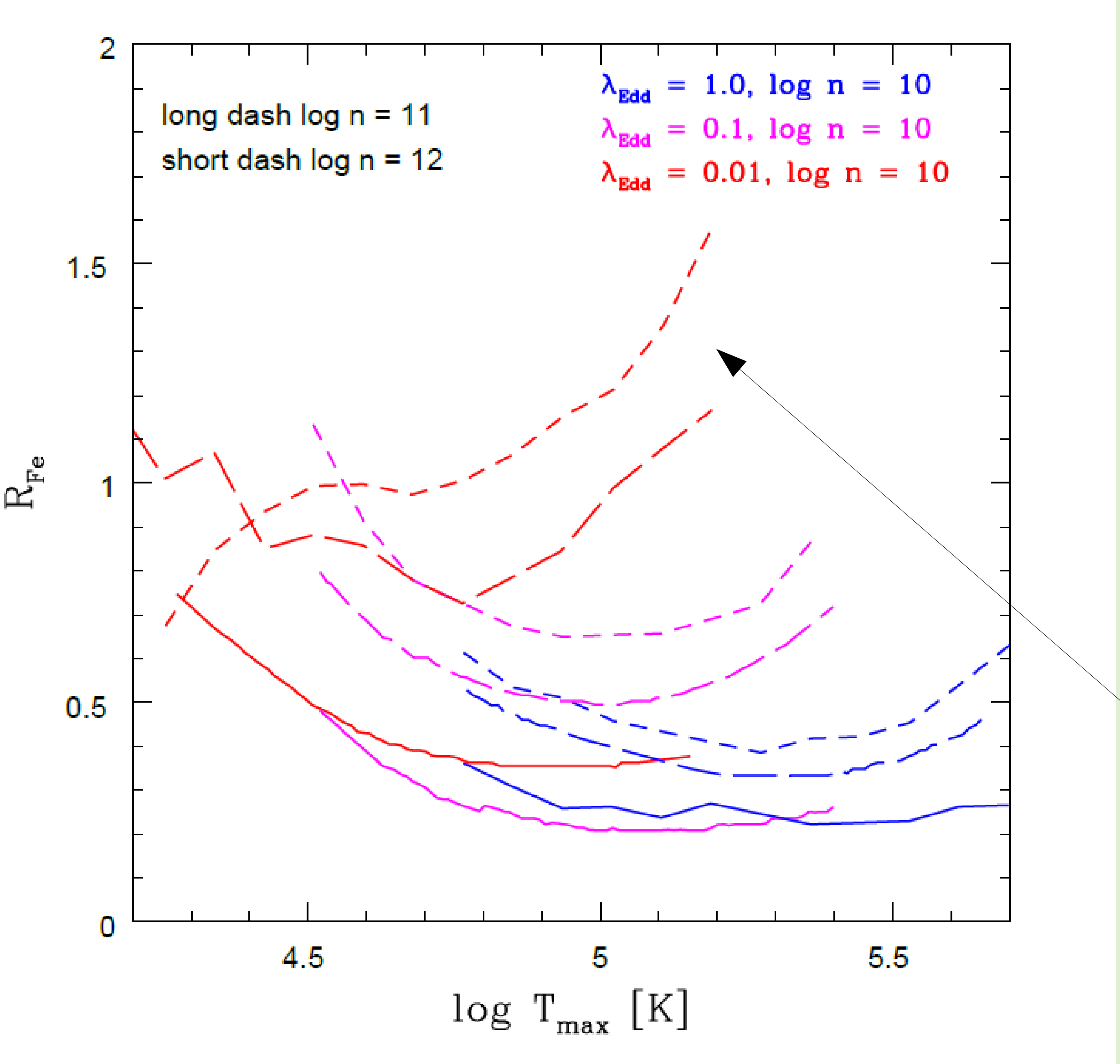


Mean quasar parameters from SDSS Shen et al. (2011) catalog are well represented.

Relatively large values of R_Fe are populated by the high density **LOW EDDINGTON** ratio models...

*Panda et al. (in preparation)*

# Modelled EV1 trend

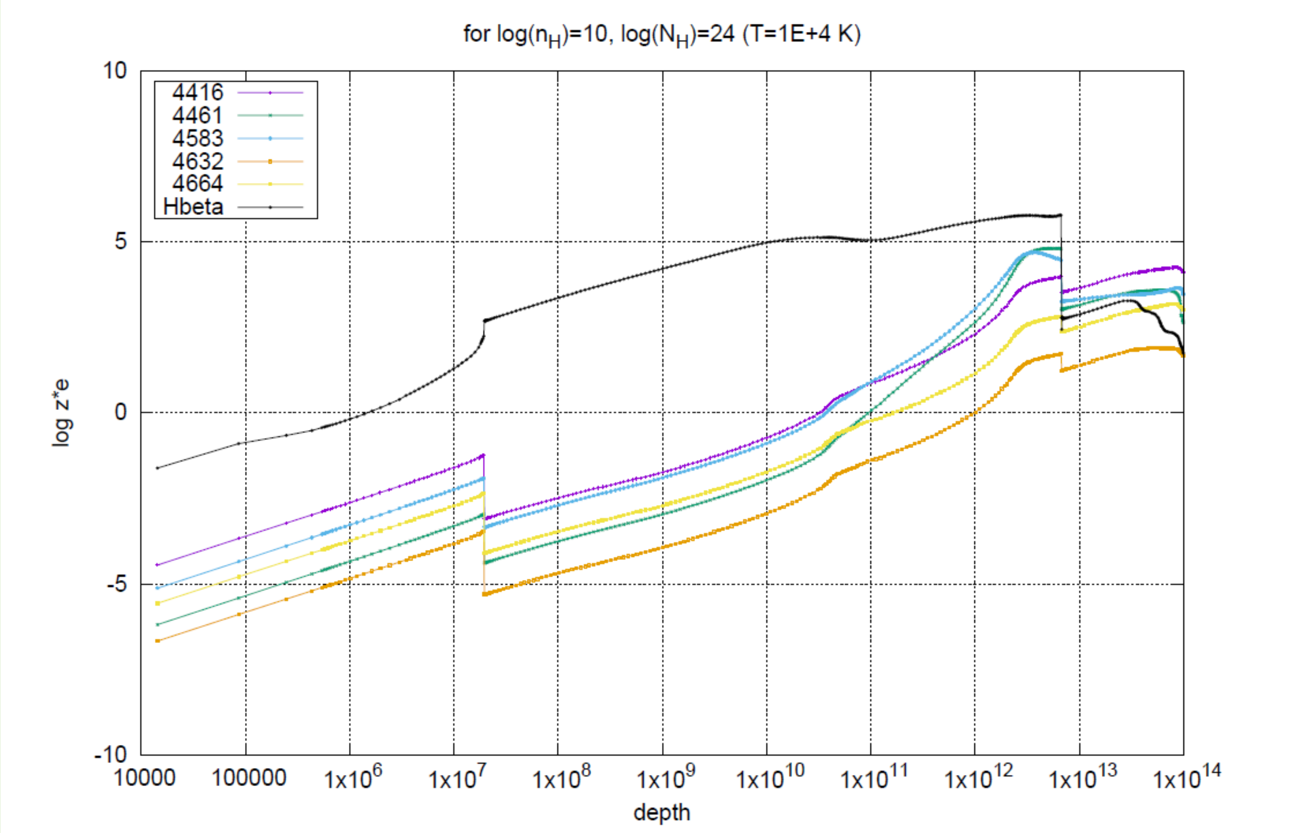


Emissivity profile within the cloud as a function of depth [cm].

Relatively large values of R_Fe are populated by the high density **LOW EDDINGTON** ratio solutions.

It may also be that we do not account properly for the dark side of the cloud if the cloud distribution is not much flattened.

*Panda et al. (in preparation)*

# Modelled EV1 trend

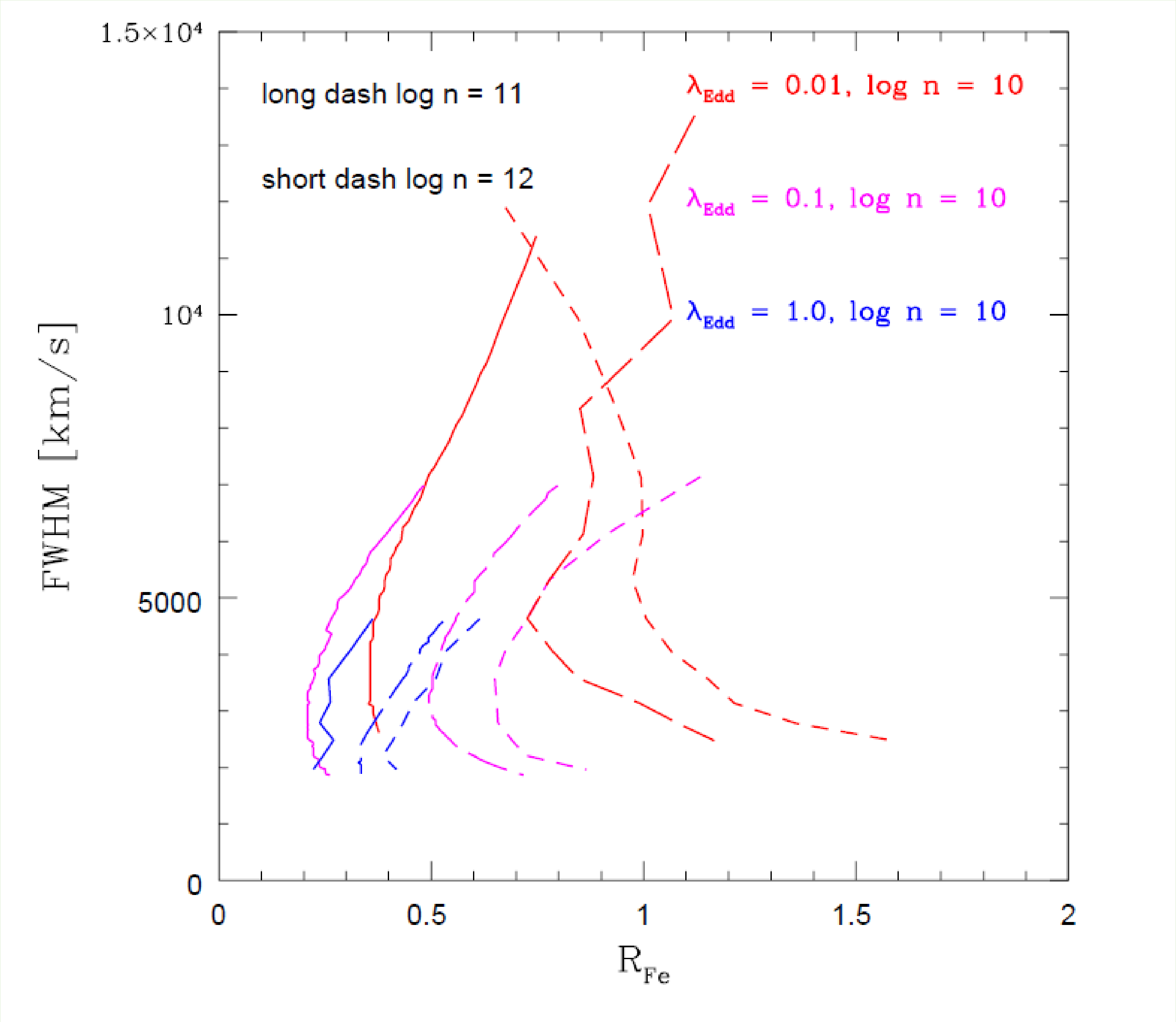


The optical plane is broadly covered. Adding additionally some turbulent velocity and changing from constant density cloud to constant pressure cloud approximation increases somewhat the values of R_Fe.

*Panda et al. (in preparation)*

# Non-monotonic dependence

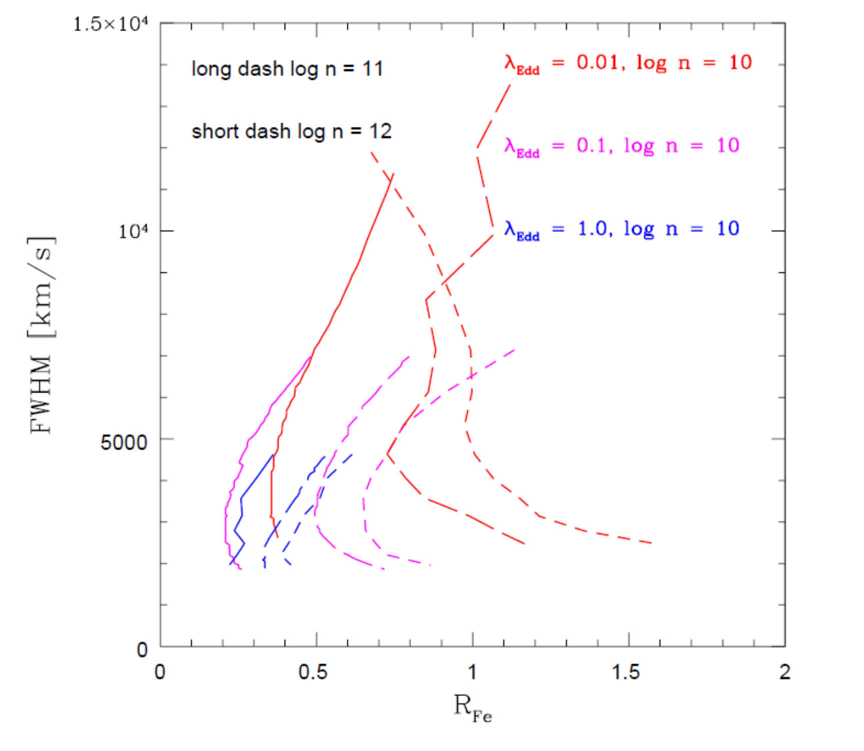


This non-monotonic dependence is convenient to explain the strong Fe II emitters both with narrow and broad lines.

However, to get systematically higher values of R_Fe for higher T_max or L/L_Edd we need

**a rise in the density and turbulent velocity with T_max or L/L_Edd.**

Similar conclusion with respect to the EV1 has been reached by Lawrence et al. (1997), and they connected the density of the material with the density of the outflowing wind.

# Density issue

The clear division between BLR and NLR is due to the presence of dust (Netzer & Laor 1993).

In our study of existence of ILR we showed that this gap vanishes if the local density is high since the dust does not intercept significant fraction of photons while it does that at low densities.

High Eddington sources have no clear division into BLR and NLR.

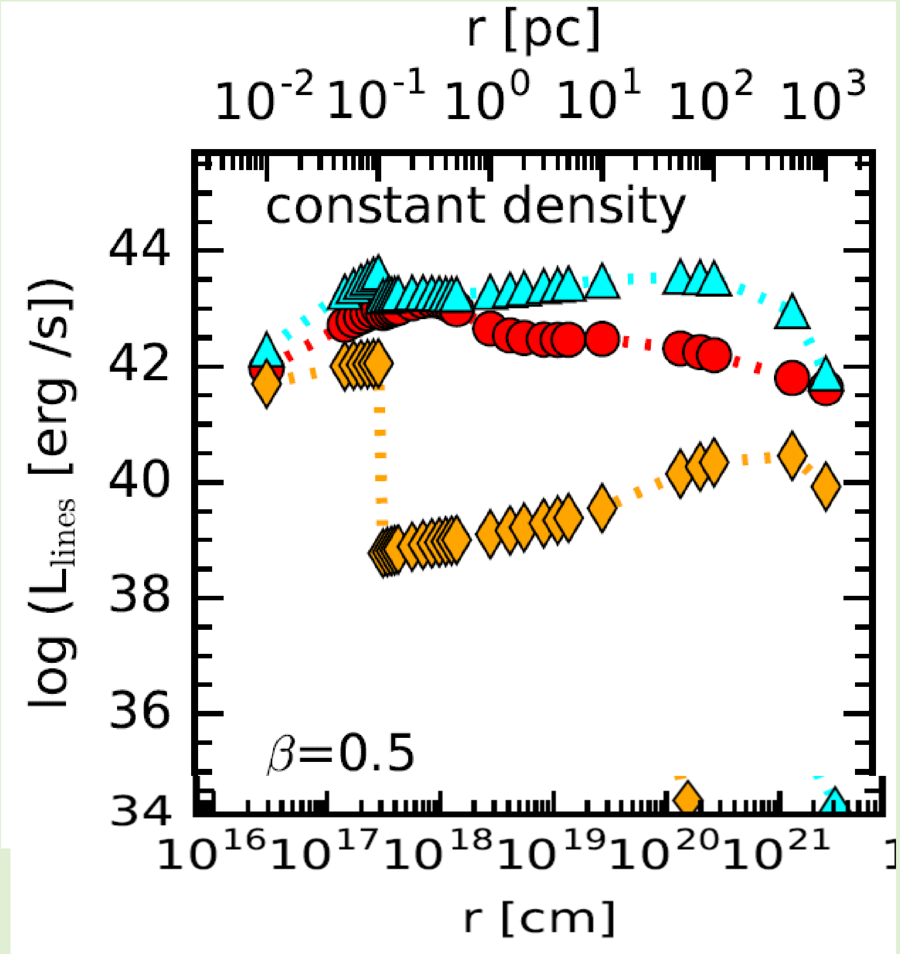


*(Adhikari et al. 2018).*

# Possible scenario. I.

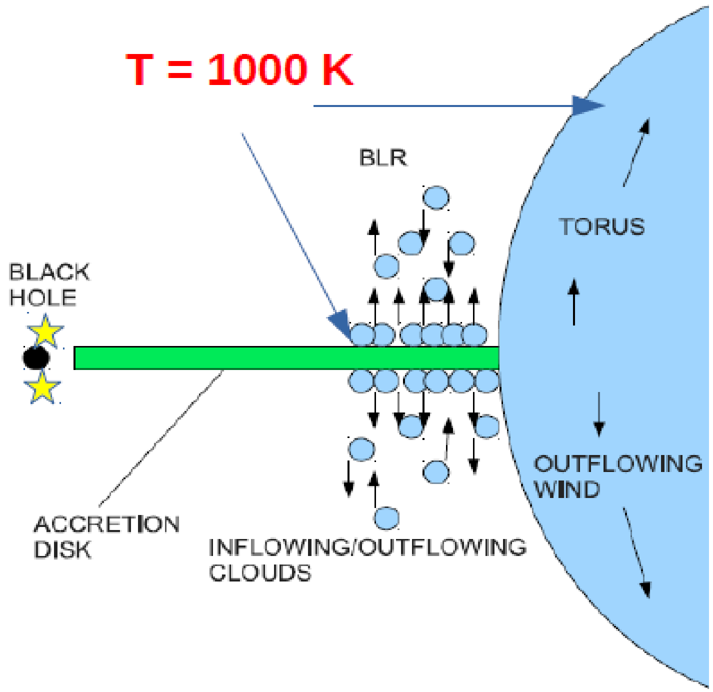


**Fig. 1.** The BLR region covers the range of the disk with an effective temperature lower than 1000 K: the dusty wind rises and then breaks down when exposed to the radiation from the central source. The dusty torus is the disk range where the irradiation does not destroy the dust

## Theory outlined in Czerny & Hryniewicz (2011):

- Large outflow forms in the region where the disk temperature is below 1000 K and allows for dust formation
- Ouflow is caused by radiation pressure acting on dust grains
- Far from the disk the dusty clouds are irradiated and dust evaporates
- Dustless material looses support against gravity and falls back
- Failed wind forms

**FRADO – Failed Radiatively Accelerated Dusty Outflow**

# Possible scenario. II.

In this model the scale height of the clouds is set by

$$z_* = \frac{3\dot{M}\sigma_{dust}}{8\pi mc}.$$

and the time spend on the rise and fall scales with the local Keplerian period which, combined with R_BLR size gives

Period propto (mdot/M)$^{1/2}$

So it is longer for sources with higher Eddington ratio and smaller mass. The material has more time to get clumpy.

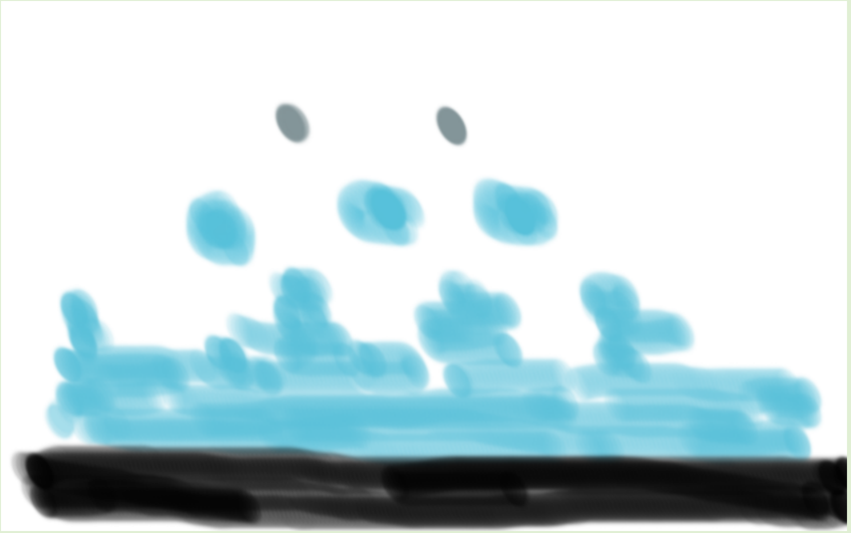

The possible problem: high Eddington ratio sources are 'softer' and the thermal instability may not work efficiently enough to make the medium clumpy.

# Attempts at UV plane

We tried to make a similar to the optical plane but using Mg II (also Low Ionization Line) and UV Fe II.

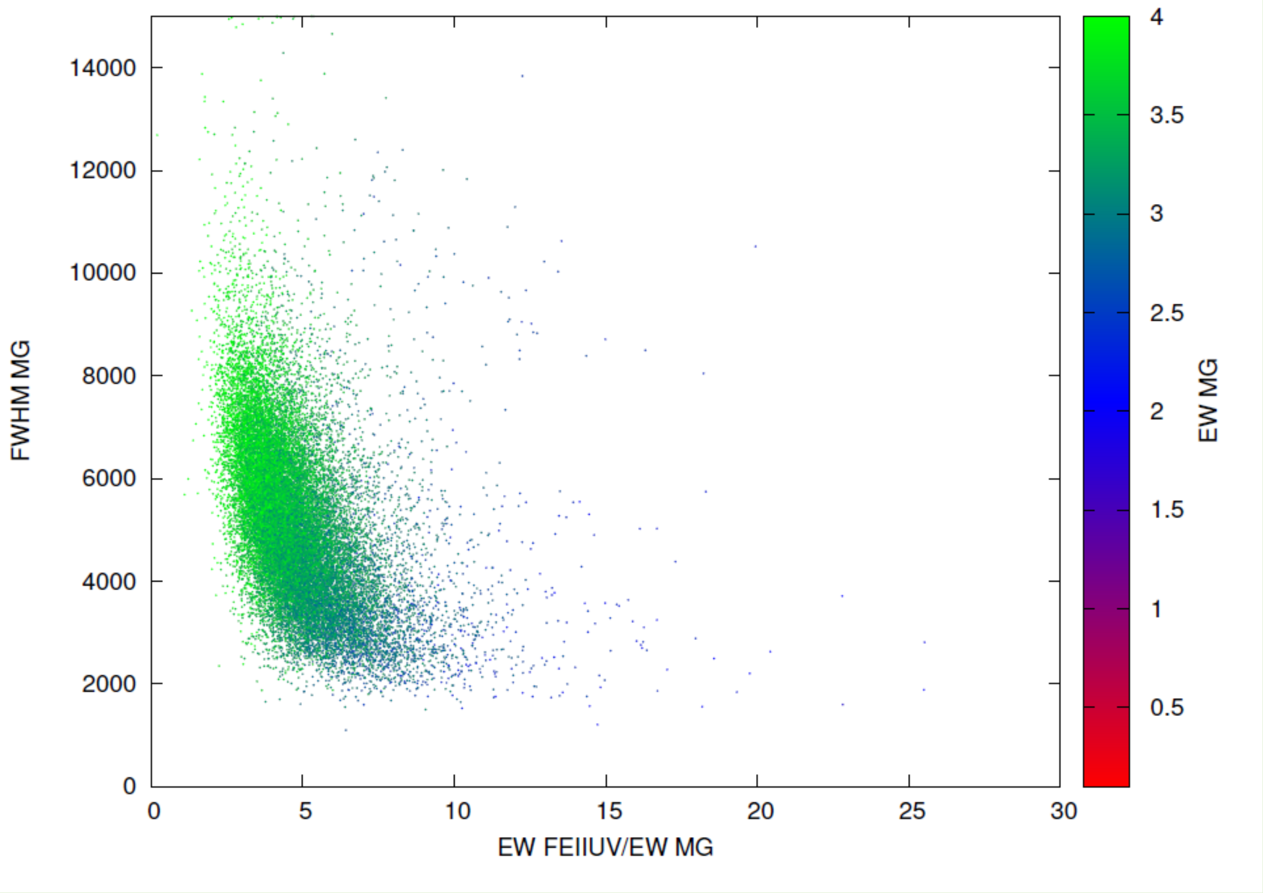


*Śniegowska et al, in preparation*

# Attempts at UV plane

We tried to make a similar to the optical plane but using Mg II (also Low Ionization Line) and UV Fe II. But the correlation is apparently driven only by a strong trend in Mg II itself, and not by trend in Fe II.

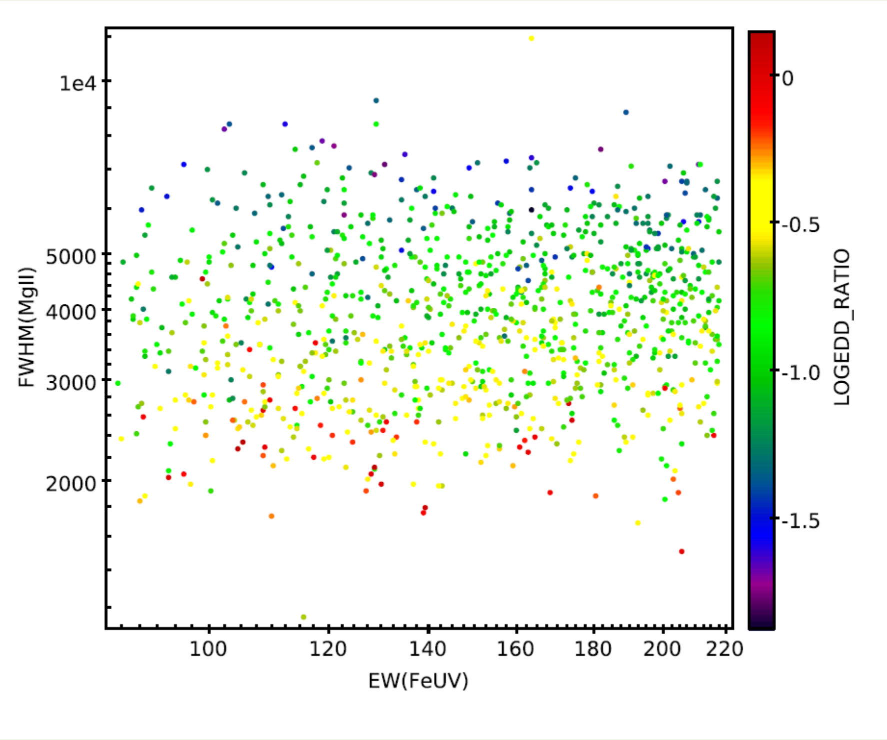


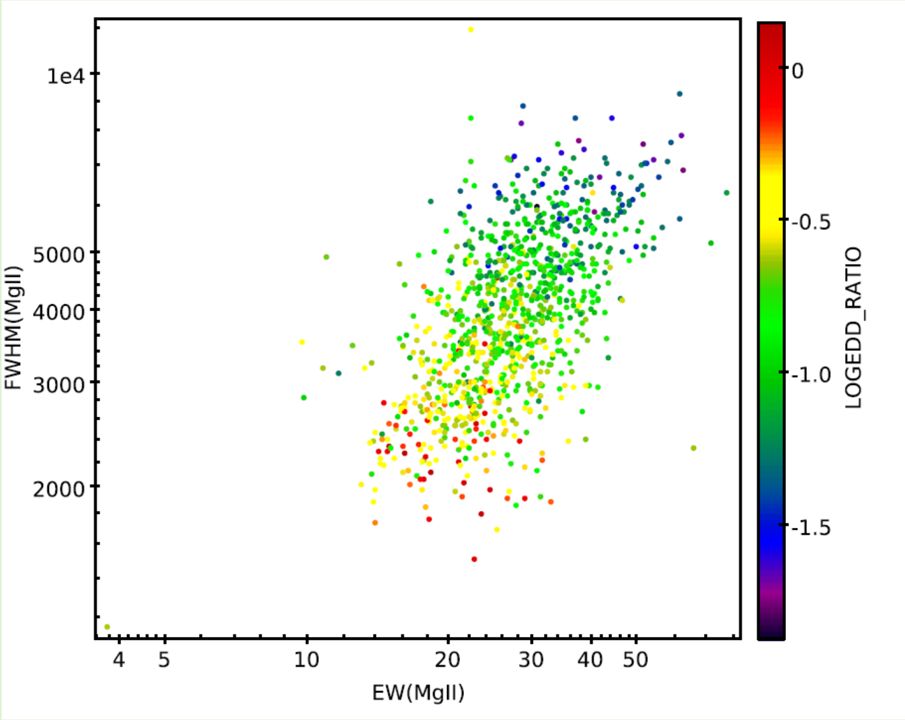


*Śniegowska et al, in preparation*

# Summary

- Divisions into NLS1/S1 or type A/type B quasars can be used only after statement about the mass range explored, preferentially narrow (see also talk by Paola Marziani), and frequently they can be confusing

- Studies of the optical plane without supplementing info from X-rays are difficult since we miss the direct link to the broad band SED (again, see ideas of Marziani, Sulentic,…)

- The density is the possible driver of the quasar main sequence; if so, the connection to basic parameters (black hole mass, accretion rate, spin, inclination) would be indirect

- Direct modelling of Fe II production is promising but needs more advanced scenario